Chapter 11
Post-failure Processes on the Continental Slope of the Central Nile Deep-Sea Fan: Interactions Between Fluid Seepage, Sediment Deformation and Sediment-Wave Construction

Sébastien Migeon, Silvia Ceramicola, Daniel Praeg, Emmanuelle Ducassou, Alexandre Dano, João Marcelo Ketzer, Flore Mary, and Jean Mascle

Abstract Voluminous mass-transport deposits (MTD) have been identified on seismic profiles across the central Nile Deep-Sea Fan (NDSF). The youngest MTDs are buried under 30–100 m of well-stratified slope deposits that, in water depths of 1,800–2,600 m, are characterized by undulating reflectors correlated with slope-parallel seabed ridges and troughs. Seabed imagery shows that, in the western part of the central NDSF, short, arcuate undulations are associated with fluid venting (carbonate pavements, gas flares), while to the east, long, linear undulations have erosional furrows on their downslope flanks and fluid seeps are less common. Sub-bottom profiles suggest that the western undulations correspond to rotated fault-blocks above the buried MTDs, while those in the east are sediment waves generated by gravity flows. We suggest that fluids coming from dewatering of MTDs and/or from deeper layers generate overpressures along the boundary between MTDs and overlying fine-grained sediment, resulting in a slow downslope movement of the

S. Migeon (✉) • A. Dano
Géoazur, UMR7329, UNS-UPMC-CNRS-OCA, Rue Albert Einstein, 06560 Valbonne, France
e-mail: migeon@geoazur.unice.fr

S. Ceramicola • D. Praeg
OGS (Istituto Nazionale di Oceanografia e di Geofisica Sperimentale), Borgo Grotta Gigante 42c, 34010 Trieste, Italy

E. Ducassou
Université Bordeaux 1, UMR5805 EPOC, Av. des facultés, 33405 Talence cedex, France

J.M. Ketzer
Center of Excellence in Research and Innovation in Petroleum, Mineral Resources and Carbon Storage (CEPAC), Pontifical University of Rio Grande do Sul (PUCRS), Av. Ipiranga 6681, Prédio 96J, CEP 90619-900, Porto Alegre-RS-, Brazil

F. Mary
UMR7329 Géoazur, UPMC-UNS-CNRS-OCA, rue A. Einstein, 06560 Valbonne, France

J. Mascle
Géoazur, UMR7329, UNS-UPMC-CNRS-OCA, Porte de la Darse, Villefranche-sur-Mer, France

S. Krastel et al. (eds.), *Submarine Mass Movements and Their Consequences*, Advances in Natural and Technological Hazards Research 37, DOI 10.1007/978-3-319-00972-8_11,

sediment cover and formation of tilted blocks separated by faults. Fluids can migrate to the seafloor, leading to the construction of carbonate pavements. Where the sediment cover stabilizes, sediment deposition by gravity flows may continue building sediment waves. These results suggest that complex processes may follow the emplacement of large MTDs, significantly impacting continental-slope evolution.

Keywords MTDs • Sediment waves • Deformation • Fluid seepages

11.1 Introduction

Gravity-driven sediment failure is an ubiquitous process on continental margins, resulting in a wide range of possible morpho-sedimentary expressions (McAdoo et al. 2000; Canals et al. 2004). Most studies of submarine landslides have concentrated on the triggering and dynamics of failures and their impacts as geohazards. In contrast, less attention has been given to processes following the emplacement of landslides on continental slopes. Although slope failures are known to decrease slope angles, which should inhibit further landslides, it has been shown that a return to stable conditions may involve several processes of erosion/deposition (Joanne et al. 2010). Moreover, observations of fluid seeps in the vicinity of slide scars raises the question of their role prior to and/or following failure (e.g. Lastras et al. 2004).

In this study, we examine sedimentary records of post-failure activity in the central Nile Deep-Sea Fan (NDSF), using a large dataset including multibeam seabed imagery, seismic-reflection profiles, and deep-towed side-scan sonar and 2–5 kHz data collected during the FANIL (2001) and APINIL campaigns (2011). Previous studies of the NDSF have shown its stratigraphic architecture to be characterised by large Mass-Transport Deposits (MTDs) (Garziglia et al. 2008; Loncke et al. 2009). In the central NDSF, stratified sediments form slope-parallel seabed undulations interpreted to record slope destabilisation in association with widespread fluid seepage, the latter recorded by high-backscatter carbonate pavements (Bayon et al. 2009). Here we present a first examination of lateral variability in the character of the undulations and fluid seeps, and consider it in relation to the interaction of processes of deformation and downslope deposition.

11.2 Methods

Multibeam bathymetric and backscatter data were acquired using hull-mounted Simrad EM300 and EM302 systems during the FANIL and APINIL campaigns, respectively. In the water depths of interest (1,800–2,600 m), the EM300 resulted in DTMs with a spatial resolution of 50 m (bathymetry) and 25 m (backscatter), while the EM302 yielded higher resolution DTMs of 25 m (bathymetry) and 10 m (backscatter). Subbottom profiles were acquired during both campaigns using a hull-

mounted chirp system. During the APINIL campaign, a deep-towed acoustic system (*Système Acoustique Remorqué*: SAR) deployed c. 70 m above the seabed provided both sidescan sonar imagery (resolution of 25 cm across swaths up to 1 km wide) and 2–5 kHz profiles (vertical resolution of 80 cm). Deeper penetration seismic-reflection profiles were acquired during FANIL using a 24-channel streamer and 2 mini-GI guns.

11.3 Results

Due to suspected interaction between buried bodies and seafloor features, we first describe the continental-slope architecture then the main seafloor morphologies.

11.3.1 Architecture and Age of MTDs and Slope Deposits

Seismic-reflection profiles show the upper 400 ms of the central NDSF to be characterised by up to 10 stacked lenticular bodies with a chaotic acoustic facies, interpreted as MTDs, and interbedded with high-amplitude reflection packages interpreted as turbidite channels (Fig. 11.2). The MTDs are 22–220 m (20–200 ms) thick, with sharp or erosive basal contacts and irregular tops. The youngest (MTD13) is about 150-km long and 35-km wide (Figs. 11.1 and 11.2; Rouillard 2010) and corresponds in cores to a debrite facies dated at c. 73 kyrs (Ducassou et al. 2013). MTD13 is buried by a stratified seismic facies 33–55 m (30–50 ms) thick (Fig. 11.2), corresponding in cores to alternating hemipelagite and turbidite deposits (Ducassou et al. 2009). To the east across the central NDSF, the stratified facies thickens up to 110 m above buried MTDs of unknown age but older than MTD13 (Fig. 11.2).

11.3.2 Seabed Sediment Undulations

Multibeam data show the seafloor of the central NSDF across water depths of 1,800–2,600 m to be dominated by sediment undulations, comprising elongate ridges alternating with trough-like depressions (Fig. 11.1). From east to west across a field of about 3,400 km^2, a clear change is observed in both the plan-form morphology and internal architecture of the undulations.

In the eastern part of the field, the mean slope angle is $\leq 0.8°$ and undulations are mainly slope-parallel (Fig. 11.1). Ridge crests are continuous for 2–9 km; most are linear and parallel with consistent wavelengths of 0.5–1 km, although some are arcuate and convex upslope or downslope in plain view. Ridges are 10–20 m high on the upper slope and decrease downslope to ≤ 5 m. In cross-section, the ridges

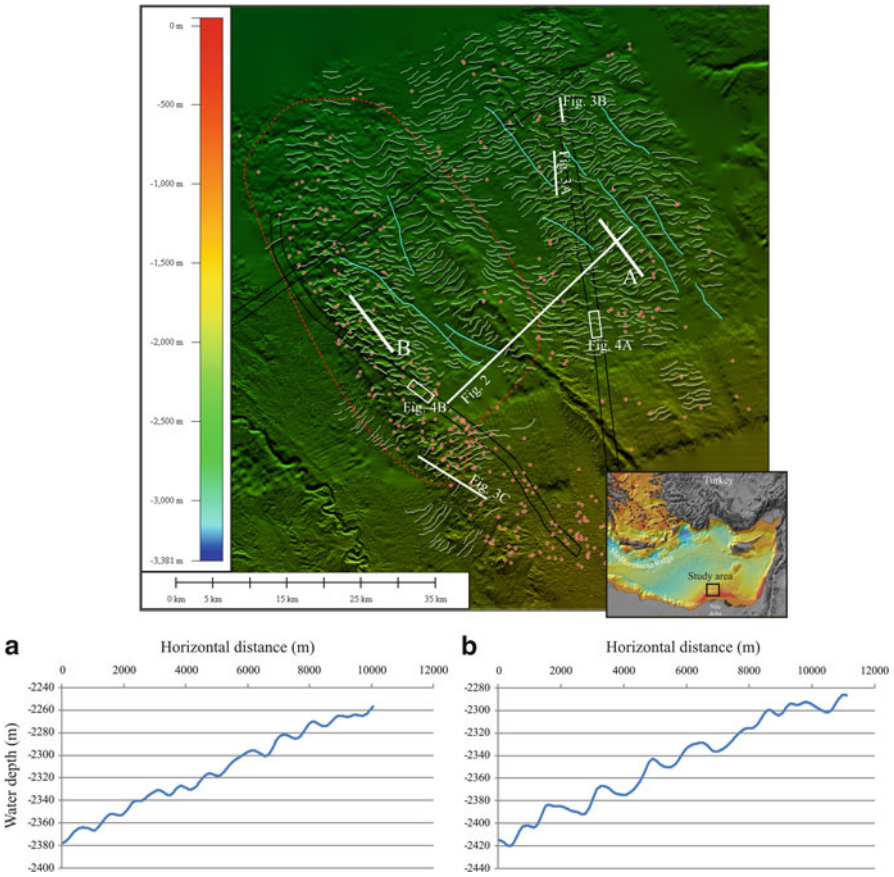

Fig. 11.1 Bathymetric map of the study area in the central NDSF. *Red dots* are multibeam high-backscatter patches. *White continuous lines* display crests of seabed undulations. *Blue lines* are small sediment pathways. The *red dashed line* displays the limit of MTD13. (**a**) and (**b**) are topographic profiles. The inset shows location of the study area on the Nile margin

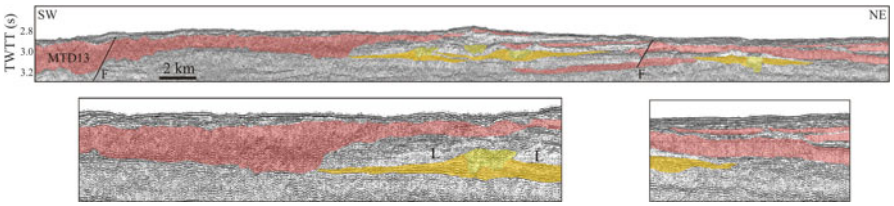

Fig. 11.2 Seismic profile illustrating occurrence of buried MTDs (*red bodies*) in the central NDSF. Some MTDs are affected by faults (*F*). *Yellow and orange bodies* are turbidite-channel infillings with adjacent levees (*L*). Profile location shown on Fig. 11.1

are mostly asymmetrical, with shorter upslope flanks (Figs. 11.1, and 11.3a, b), but symmetrical undulations also occur. In profile, the ridges consist of a well-layered echofacies, the first 30 ms of which thickens on upslope flanks, indicating higher sediment deposition, and thins on downslope flanks where truncations are common, indicating reduced deposition or erosion (Fig. 11.3a, b). Thus these structures have migrated upslope through time (Fig. 11.3a, b). They overlie a disorganized unit in which reflectors are tilted, disrupted and shifted vertically by faults (Fig. 11.3a). This unit overlies a MTD (Figs. 11.2, and 11.3a) which top itself exhibits relief (Fig. 11.3a). Sidescan sonar imagery across most of ridges (downslope flanks) reveal abundant furrows, 300–500-m long and 10–20-m wide, oriented parallel or oblique to slope (Fig. 11.4a), suggesting recent seafloor erosion by downslope flows.

In the western part of the field, overall slope angles are about 2.5° and in places up to 5.2°. The undulations are mainly arcuate and oriented oblique (10–40°) to slope, exhibiting a heterogeneous plan-form organisation that changes westwards (Fig. 11.1). In the eastern area of the western part, most arcuate crests are convex downslope; they are subparallel and up to 3 km long, with wavelengths of 1–1.5 km, and heights of 10–20 m with no downslope change. In the western area, most ridges are disrupted and <1 km long, with sharp changes of orientation (Fig. 11.1); they are 5–10 m high and ≤ 500 m in wavelength and distributed randomly along the slope (Fig. 11.1). In some places, they display a blocky pattern, more chaotic to the west. In profile, ridges are mainly asymmetrical with shorter and steeper downslope flanks (Figs. 11.1 and 11.3c), the reverse of the eastern part of the field, but also include symmetrical shapes with flat tops. Subbottom reflectors are continuous between adjacent ridges (Fig. 11.3c), parallel to seafloor and slightly wavy with wave amplitude constant with depth (Fig. 11.3c). Sediment thickness is nearly constant between reflectors across the ridges, providing no evidence for upslope or downslope migration (Fig. 11.3c). Small vertical offsets in reflectors across some troughs suggest faulting processes (Fig. 11.3c). Troughs are characterized by higher-amplitude reflections vertically aligned and resembling chimney-like structures (Fig. 11.3c; Loncke et al. 2004). Sidescan sonar imagery show the troughs to contain abundant intermediate-backscatter elongate patches trending parallel to the trough orientation, as well as smaller numbers of high-backscatter rounded patches (Fig. 11.4b), both inferred to be carbonate pavements related to gas venting (Dano et al. 2013). Gas flares identified in the water column above some of the high-backscatter patches indicate active fluid vents (Dano et al. 2013; Praeg et al. 2013). An absence of furrows suggests limited recent downslope particle transport/deposition.

11.3.3 Sediment Pathways

Several slope-perpendicular linear structures are located on the continental slope in water depths of 2,100–2,600 m (Fig. 11.1). They are 6–19-km long and V-shaped in cross section. They are interpreted as small-scale sediment-transport pathways.

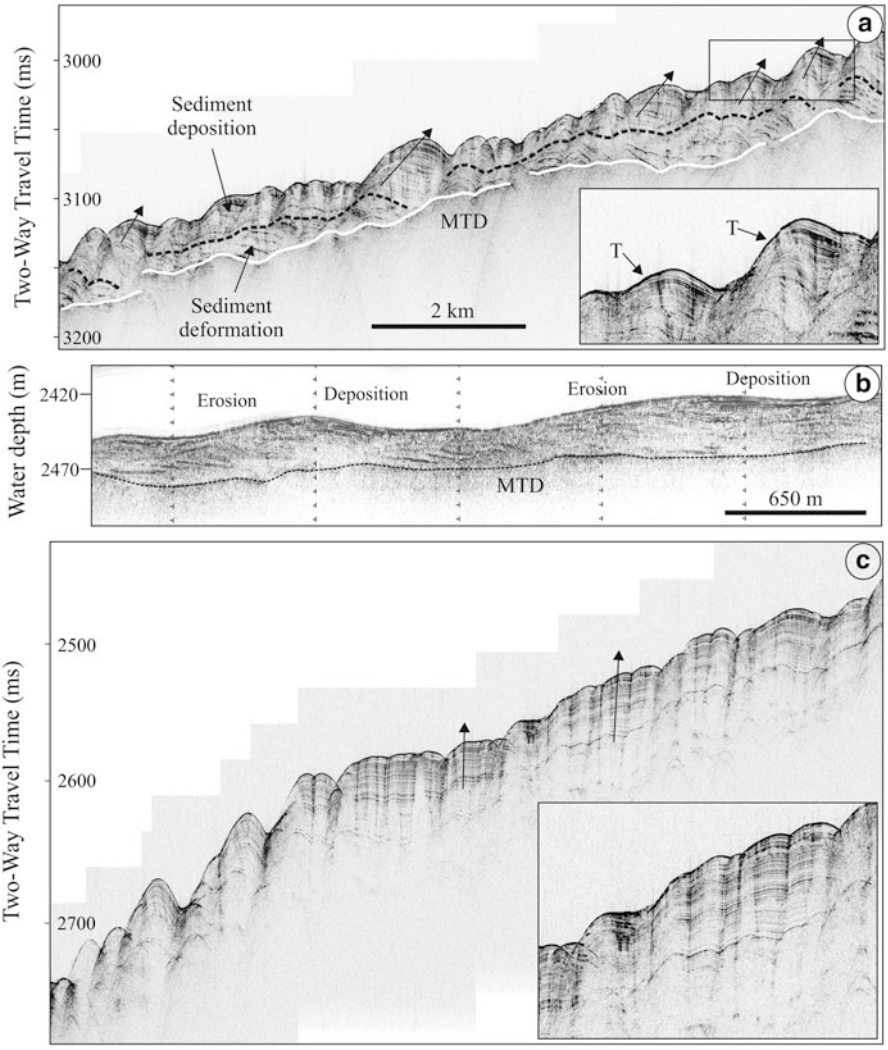

Fig. 11.3 (**a**) Hull-mounted subbottom profile illustrating sediment-waves; the *white line* is the *top* of a MTD and the *dashed line* is the *top* of a deformed interval (see text). (**b**) SAR subbottom profile illustrating sediment-waves; the *dotted line* is the *top* of a MTD. (**c**) Hull-mounted subbottom profile illustrating extensional deformations associated with fluid upward migration. Profiles location shown in Fig. 11.1

A well-developed channel-levee system (named DSF4 by Ducassou et al. 2009) is also located in the middle part of the study area, in water depths of 1,800–2,300 m (Fig. 11.1). It formed between 73 and 10 kyrs and is now being progressively buried by the undulations.

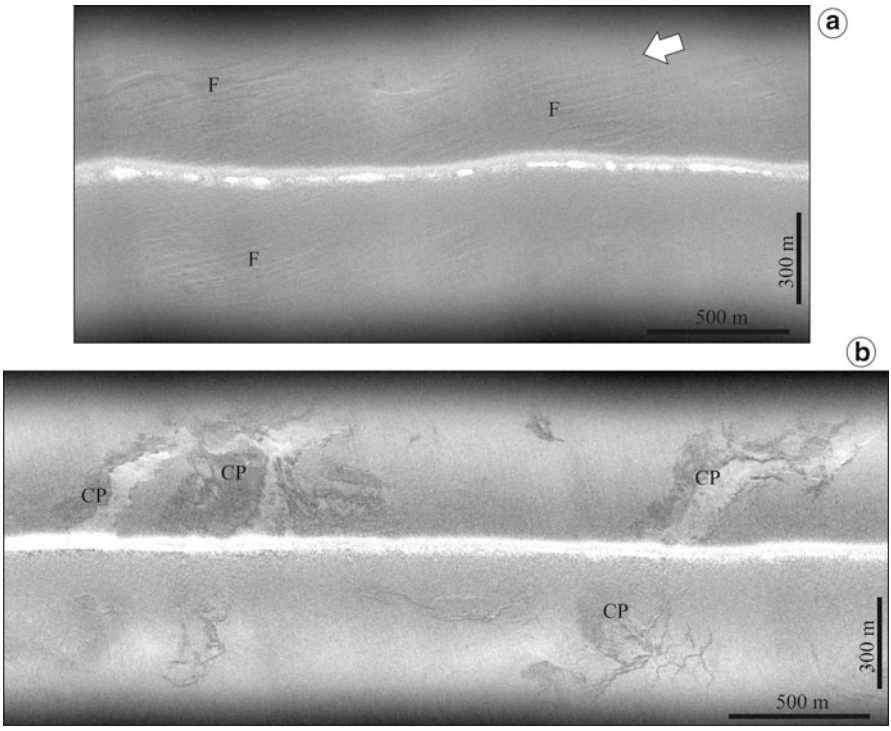

Fig. 11.4 SAR imagery illustrating (**a**) furrows (*F*) associated with sediment waves in the eastern study area, and (**b**) carbonate pavements (*CP*) flooring troughs of extensional deformations in the western study area. The *white arrow* indicates the main direction of turbulent flows that generated furrows. Images location shown in Fig. 11.1

11.4 Discussion

Undulating seabed sedimentary structures have been described on levees adjacent to turbidite channels, open continental slopes and submarine pro-deltas (Migeon et al. 2004; Hoffmann et al. 2011; Urgeles et al. 2011). They have been interpreted as either sediment waves deposited by turbulent flows, or deformation structures recording gravity-driven displacement of pre-existing sediment. The seabed undulations of the central NDSF have previously been interpreted as purely creeping/gliding features (Loncke et al. 2004; Bayon et al. 2009). We argue instead that the undulations provide evidence of both depositional and deformational processes. We first show the two main types of sediment undulations observed across the study area to correspond to end-member cases of these processes, then consider their overall relation to the underlying MTDs.

11.4.1 End-Members: Sediment Waves Versus Deformation Structures

In the eastern part of the study area, the plan-form morphology of the ridge crests and their downslope decrease in amplitude and wavelength are consistent with construction from turbulent gravity flows of decreasing velocity and particle load downslope (Normark et al. 2002). The presence of furrows on the downslope flanks of ridges confirms the role of these flows, at least during recent times, as does the occurrence of small-scale sediment pathways (Fig. 11.1). At the scale of individual ridges, the activity of successive turbulent flows caused preferential sediment deposition on their upslope flanks and by-passing or erosion of their downslope flanks (Fig. 11.3a), leading to upslope migration of the ridges. A similar pattern was observed in other slope settings, resulting in comparable slope-parallel sediment waves built by turbidity currents (Migeon et al. 2001; Normark et al. 2002).

In the western part of the study area, the chaotic convex-downslope morphology of the undulations, their 'reversed' asymmetry and absence of furrows suggest a limited impact of gravity flows in their formation. Their internal architecture provides no evidence of migration over time (Fig. 11.3c), consistent with either low-energy depositional draping of a pre-existing wavy topography, or with extensional deformation of the sediment cover. The presence of faults beneath the intervening troughs, many associated with gas seepage (Figs. 11.3c and 11.4b), favours the role of post-depositional rotational movements generated along shallow normal faults, as noted by previous authors (Loncke et al. 2004; Bayon et al. 2009).

The end-member cases of sediment-wave construction and extensional deformation are not exclusive. Thus in the eastern part of the study area, rotational structures are observed at depth (Fig. 11.3a), sandwiched between the undulating seabed sediments and the top of the MTD, suggesting that extensional deformation following MTD emplacement provided the pre-existing morphology that led to sediment-wave growth, as has been described in other areas (Hoffmann et al. 2011). In contrast, in the western part of the study area, sediment geometries continue to be dominated by extensional deformation involving rotating fault blocks, with widespread fluid venting along troughs aligned with fault planes.

11.4.2 Post-failure Slope Evolution

This work suggests that across the central NDSF, the formation of undulating sediment structures is initially linked to extensional deformation following the emplacement of large MTDs. Many extensional faults root within the MTDs and could result from differential compaction of these deposits, while others only affect

the overlying sediment cover and suggest slow gliding above MTDs. Because MTDs are younger and shallower to the west and the sediment cover thickens to the east (Fig. 11.2), extensional features should not be synchronous over the study area but must become younger to the west. Thus the west-east transition from irregular extensional features to well-developed sediment waves could reflect the increasing age of post-MTD processes affecting the slope.

After the emplacement of a large MTD, new sediment pathways develop on the slope and facilitate the deposition of a sediment drape. With time, the MTD experiences compaction, dewatering and eventual fluid release. Overpressures generated between the MTD and the overlying fine-grained sediment cover could then facilitate the slow gliding of the sediment cover along extensional faults rooting in the MTD. However, fluid seepage taking place across the central NDSF are also likely to be derived from deeper layers, including suspected gas hydrates (Praeg et al. 2008). This suggests another hypothesis that gas may accumulate at the base of an MTD, forming an overpressured horizon that contributes to the deformation of the overlying (and thickening) sediment mass and the development of fluid migration pathways allowing gas release.

In either case, rotational movements must be favoured by upward fluid flow along faults acting as conduits (Dano et al. 2013; Praeg et al. 2013). At seabed, gas-rich fluids lead to the construction of carbonate pavements. Carbonate precipitation may also take place within the conduits characterized by high-amplitude reflections (Fig. 11.3c). Such a process is thought to increase the cohesion of deposits and could contribute to the progressive stabilization of the sediment cover. Where sediment pathways exist, inactive rotational features will gradually be buried by gravity flows that may build sediment waves.

Additional high-resolution seismic profiles and 3D seismic data are now necessary to investigate the sediment cover above older MTDs to see whether this evolution is applicable or not to any time intervals.

11.5 Conclusion

An integrated analysis of multibeam and side-scan seabed imagery, and seismic profiles reveals lateral variations in the character of undulating features built on top of large MTDs across the central NDSF. They are interpreted to record the interaction of two end-member gravity-driven processes, extensional deformation associated with faulting and fluid migration, and sediment waves built by turbulent flows. Deformation features provide an initial morphology for sediment deposition and, where extension is reduced or ceases, may be progressively transformed into sediment waves. These results indicate that complex processes of continental-slope evolution may follow the emplacement of MTDs.

Acknowledgments The authors thank captains and crew of the RV Le Suroit and their colleagues present during the campaigns. The authors are thankful to Guillaume St Onge, Sam Johnson and David Völker for their reviews and constructive comments. This work was funded by the CNRS-INSU and the French program Action Marges.

References

Bayon G, Loncke L, Dupré S et al (2009) Multi-disciplinary investigation of fluid seepage on an unstable margin: the case of the Centre Nile deep sea fan. Mar Geol 26:92–104

Canals M, Lastras G, Urgeles R et al (2004) Slope failure dynamics and impacts from seafloor and shallow sub-seafloor geophysical data: case studies from the COSTA project. Mar Geol 213:9–72

Dano A, Praeg D, Migeon S et al (2013) Fluid seepage in relation to seafloor deformation on the central Nile Deep-Sea Fan, part 1: evidence from side-scan sonar data. In: Krastel S, Behrmann J-H, Völker D, Stipp M, Berndt C, Urgeles R, Chaytor J, Huhn K, Strasser M, Harbitz CB (eds) Submarine mass movements and their consequences. Advances in Natural and Technological Hazards Research 37, Springer, Heidelberg

Ducassou E, Migeon S, Mulder T et al (2009) Evolution of the Nile Deep-Sea Turbidite system during Late Quaternary: influence of climate change on fan sedimentation. Sedimentology 56:2061–2090

Ducassou E, Migeon S, Capotondi L, Mascle J (2013) Run-out distance and erosion of debris flows in the Nile deep-sea fan system: evidence from lithofacies and micropalaeontological analyses. Mar Petrol Geol 39:102–123

Garziglia S, Migeon S, Ducassou E et al (2008) Mass-transport deposits on the Rosetta province (NW Nile Dea-sea turbidite system, Egyptian margin): characteristics, distribution, and potential causal processes. Mar Geol 250:180–198

Hoffmann G, Silver E, Day S et al (2011) Deformation versus deposition of sediment waves in the Bismarck Sea, Papua New Guinea. Mass-transport deposits in deepwater settings. SEPM Spec Publ 96:455–474

Joanne C, Collot JY, Lamarche G, Migeon S (2010) Continental slope reconstruction after a giant mass failure, the example of the Matakaoa Margin, New Zealand. Mar Geol 268:67–84

Lastras G, Canals M, Urgeles R et al (2004) Shallow slides and pockmarks swarms in the Eivissa Channel, western Mediterranean Sea. Sedimentology 51:837–850

Loncke L, Mascle J, Scientific Party FANIL (2004) Mud volcanoes, gas chimney, pockmarks and mounds in the Nile deep-sea fan (Eastern Mediterranean): geophysical evidences. Mar Petrol Geol 21:669–689

Loncke L, Gaullier V, Droz L et al (2009) Multi-scale slope instabilities along the Nile deep-sea fan, Egyptian margin: a general overview. Mar Petrol Geol 26:633–646

McAdoo BG, Pratson LF, Orange DL (2000) Submarine landslide geomorphology, US continental slope. Mar Geol 169:103–136

Migeon S, Savoye B, Zanella E et al (2001) Detailed seismic-reflection and sedimentary study of turbidite sediment waves on the Var Sedimentary Ridge (SE France): significance for sediment transport and deposition and for the mechanisms of sediment-wave construction. Mar Petrol Geol 18:179–208

Migeon S, Savoye B, Babonneau N, Spy-Andersson FL (2004) Processes of sediment-wave construction along the present Zaire deep-sea meandering channel: role of meanders and flow-stripping. J Sediment Res 74:580–598

Normark WR, Piper DJW, Posamentier H, Pirmez C, Migeon S (2002) Variability in form and growth of sediment waves on turbidite channel levees. Mar Geol 192:23–58

Praeg D, Geletti R, Mascle J, Unnithan V, Harmegnies F (2008) Geophysical exploration for gas hydrates in the Mediterranean Sea and a bottom-simulating reflection on the Nile Fan. In: Riassunti Estesi, 27° Convegno Nazionale GNGTS, Trieste, Italy, pp 467–469

Praeg D, Ketzer JM, Augustin AH, et al (2013) Fluid seepage in relation to seafloor deformation on the central Nile Deep-Sea Fan, part 2: evidence from multibeam and sidescan imagery. In: Krastel S, Behrmann J-H, Völker D, Stipp M, Berndt C, Urgeles R, Chaytor J, Huhn K, Strasser M, Harbitz CB (eds) Submarine mass movements and their consequences. Advances in Natural and Technological Hazards Research 37, Springer, Heidelberg

Rouillard P (2010) Modèles architectural et lithologique des dépôts quaternaires du système de Rosetta (Delta Profond du Nil, Méditerranée orientale) : implication pour un analogue actuel de réservoirs pétroliers. PhD thesis, University of Nice-Sophia Antipolis, 421 pp

Urgeles R, Cattaneo A, Puig P et al (2011) A review of undulated sediment features on Mediterranean prodeltas: distinguishing sediment transport structures from sediment deformation. Mar Geophys Res 32:49–69